HHS Public Access

Author manuscript

Biochemistry. Author manuscript; available in PMC 2020 February 12.

Published in final edited form as:

Biochemistry. 2019 February 12; 58(6): 665–678. doi:10.1021/acs.biochem.8b00716.

Stuffed Methyltransferase Catalyzes Penultimate Step of Pyochelin Biosynthesis

Trey A. Ronnebaum[1], **Jeffrey S. McFarlane**[2], **Thomas E. Prisinzano**[3], **Squire J. Booker**[4], and **Audrey L. Lamb**[1,2]

[1]Department of Chemistry, The University of Kansas, Lawrence, Kansas 66045, United States

[2]Department Molecular Biosciences, The University of Kansas, Lawrence, Kansas 66045, United States

[3]Department of Medicinal Chemistry, The University of Kansas, Lawrence, Kansas 66045, United States.

[4]Department of Chemistry, Department of Biochemistry and Molecular Biology, and the Howard Hughes Medical Institute, The Pennsylvania State University, University Park, Pennsylvania, 16802.

Abstract

Nonribosomal peptide synthetases use tailoring domains to incorporate chemical diversity into the final natural product. A structurally unique set of tailoring domains are found to be stuffed within adenylation domains and have only recently begun to be characterized. PchF is the NRPS termination module in pyochelin biosynthesis and includes a stuffed methyltransferase domain responsible for *S*-adenosylmethionine (AdoMet) dependent *N*-methylation. Recent studies of stuffed methyltransferase domains propose a model in which methylation occurs on amino acids after adenylation and thiolation rather than after condensation to the nascent peptide chain. Herein, we characterize the adenylation and stuffed methyltransferase didomain of PchF through the synthesis and use of substrate analogs, steady-state kinetics, and onium chalcogen effects. We provide evidence that methylation occurs through an S_N2 reaction after thiolation, condensation, cyclization and reduction of the module substrate cysteine and is the penultimate step in pyochelin biosynthesis.

Graphical Abstract

Corresponding Author: Audrey L. Lamb, lamb@ku.edu, phone: (785) 864-5075.

Supporting Information

Possible biosynthetic strategies for PchF (Figure S1), Separation of $HPT_{ox}T_{red}$-CO_2Et diastereomers on CHIRALCEL OD-H column (Figure S2), Adenylation assays (Figure S3), Methylated Product Formation Assays (Figure S4), $HPT_{ox}T_{red\text{-}M}$-CO_2Et standard curve (Figure S5), S-adenosylmethionine Formation Assay UPLC traces (Figure S6).

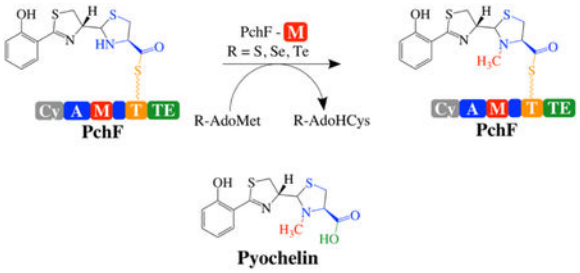

Introduction

Bacteria, fungi, and plants generate siderophores, small molecules with high affinity for ferric iron, to scavenge the surrounding environment during times of iron starvation. Indeed, many siderophores have been identified as virulence factors in pathogenic bacteria due to the metal-limiting environment of the host species. Siderophores are classified by the chemical nature of the oxygen involved in ferric iron coordination.[1] Pyochelin is a phenolate siderophore from *Pseudomonas aeruginosa,* a commensal and opportunistic gram-negative pathogen, notorious for causing infections in immunocompromised patients, burn-wound victims, and lung infections of cystic fibrosis patients.[2-5]

The precursors of pyochelin are chorismate and two cysteine molecules (Figure 1A*).*[6-8] Chorismate, from the shikimate pathway, is converted to salicylate in two steps, and is the initiating hydroxy acid. The cysteine molecules are added in succession by nonribosomal peptide synthetases (NRPSs), forming peptide bonds.[6] Encoded within the *pch* operon are tailoring domains, which perform the epimerization, reduction and methyltransferase activities required to make the final bioactive compound.[6,9-11] Pyochelin is a tricyclic acid: the 2'-hydroxyphenyl (HP) ring derived from salicylate attached to a thiazoline (T) ring from one cyclized and epimerized cysteine, followed by a methylated 4'-thiazolidine ($T_{red\text{-}M}$) heterocycle from the second cyclized cysteine.

NRPSs are multi-domain, multi-catalytic proteins arranged in modules to activate and add one substituent each to the growing chain, with each module containing a condensation or cyclization domain, an adenylation domain and a thiolation domain. The NRPS assembly line uses a 4'phosphopantetheinyl (Ppant) thiotemplate tethering system reminiscent of polyketide and fatty acid biosynthesis. This means that the peptide bond forming and tailoring chemistries are performed while the intermediates are covalently attached to a thiolation domain. The NRPS tailoring domains are affiliated with particular modules in several geometries. The most studied geometry has the tailoring domain included at the end of a module following the thiolation domain, as an independent domain that works *in cis* with the peptide bond forming domains of the module. Pyochelin biosynthesis lacks this type of tailoring domain. Some tailoring domains are stand-alone: independently expressed proteins acting *in trans,* such as the reductase of pyochelin biosynthesis (PchG).[11] Finally, there are tailoring domains that are incorporated within the adenylation domain.[12] Adenylation domains activate the substrate and attach it to the thiotemplate tethering system. The "stuffed" tailoring domains replace a loop within an adenylation domain, making a true di-domain (Figure 1B).[13] Pyochelin biosynthesis uses two stuffed tailoring domains. The

first is an adenylation-epimerase didomain in the protein named PchE, and the second is an adenylation-methyltransferase didomain in PchF.[10, 12-14]

Examples of stuffed tailoring domains, also known as “interrupted adenylation domains”,[12] participating in natural product biosynthesis include oxygenases (i.e. epothilone,[15] myxothiazol,[16] thuggacins)[17], ketoreductases (i.e. cereulide)[18], methyltransferases (i.e. thiocoraline,[1,19] cyclosporine,[20] echinomycin,[21] enniatins,[22] micacocidin,[23] microcystin,[24] pyochelin,[9, 10] yersiniabactin[9]), and epimerases (i.e. pyochelin,[9, 10] yersiniabactin[9]). Importantly, some of the natural products synthesized using stuffed tailoring domains have been isolated and experimentally show anticancer (i.e. epothilone, thiocoraline, echinomycin), antifungal (i.e. myxothiazol), antibacterial (i.e. myxothiazol, thuggacin, micacocidin), or immunosuppressive (i.e. cyclosporine) activity. However, the mechanistic and structural characterization of stuffed tailoring domains has only just begun.

Recently, mechanistic and structural studies of the stuffed methyltransferase domains from the biosynthesis of the microbial depsipeptides thiocoraline and kutzneride have been reported.[19,25-27] A main goal of these studies was to determine when in the biosynthetic pathway methylation occurs, with four possibilities: methylation of 1) the free amino acid, 2) the aminoacyl-AMP intermediate (after the amino acid is activated by ATP in the adenylation domain), 3) after thiolation (after the amino acid is attached to the Ppant tether of the thiolation domain), or 4) after condensation to the upstream peptide. Evidence suggests that the stuffed methyltransferase does not use the free amino acid as a substrate, but rather the substrate is either the aminoacyl-AMP intermediate or the amino acid attached to the thiolation domain (after thiolation).[19,25-27] The possibility remains that methyl transfer occurs after elongation with the upstream peptide; however, thiocoraline and kutzneride are complex natural products, making intermediate analog synthesis to test the hypothesis of late stage methylation difficult. Contradictory to the proposed model, isolates observed during reconstitution assays of epothilone biosynthesis and mechanistic studies of EpoB indicate that tailoring occurs after condensation to the upstream peptide chain.[14, 15] Indeed, this is logical. Epothilone biosynthesis employs a hybrid NRPS/PKS assembly line in which EpoB, a protein encoding a single NRPS module, has a stuffed oxidase domain, which oxidizes the condensed thiazoline. The EpoB stuffed oxidase domain substrate is simply a 2-methylthiazoline attached to the Ppant of the thiolation domain.

Here, using the termination module of pyochelin biosynthesis found in the protein PchF, we test the opposing hypotheses for the order of chemistry. An order of catalytic events has been proposed in the literature (Figure 1C). The PchF adenylation domain activates the cysteine substrate and attaches the cysteine to the thiotemplate of the thiolation domain.[6] The cyclization domain of PchF links the nascent chain donated from the PchE thiolation domain (HPT) to the cysteine on the thiolation domain of PchF (HPT-Cys), and subsequently cyclizes this cysteine generating a thiazoline ring (HPTT). While still tethered to the thiolation domain of PchF, PchG reduces the second thiazoline ring generating a thiazolidine ($HPTT_{red}$). The *N*-methyltransferase stuffed domain in PchF modifies the ring to generate an *N*-methylated thiazolidine ($HPTT_{red\text{-}M}$), the final proposed synthetic step before release of the mature pyochelin ($HPTT_{rod\text{-}M}CO_2^-$) by the thioesterase. Two intermediates have been hydrolyzed from the thiotemplate tether, isolated and characterized

during pyochelin reconstitution assays: HPT-Cys and $HPTT_{rod}$-CO_2^- (Figure 1D).[6, 11] The chemical release and isolation process also produced a more stable, off-pathway product hypothesized to be the result of air oxidation: $HPT_{ox}T$- CO_2^-.[6, 11] Since none of these isolated compounds contain the *N*-methyl on the thiazolidine, the order of the steps proposed for PchF is: adenylation, thiolation, condensation, cyclization, reduction, methylation and hydrolysis. However, there are some contradictory data that suggest that methylation may proceed before reduction: labeled methyl groups, from either ^{14}C-*S*-adenosylmethionine (AdoMet) or ^{3}H-AdoMet were incorporated into the product in the absence of the reductase or NADPH.[10] Altogether, the order of catalysis, and in particular when methyl transfer occurs remains elusive, leaving four reasonable pathways: 1) before condensation, 2) before cyclization, 3) before reduction, or 4) before hydrolysis (Figure S1). Herein, we synthesized a series of substrate analogues and developed kinetic analyses for the adenylation and methyltransferase activities of PchF and PchF variants to establish the order of catalytic steps performed by PchF in pyochelin biosynthesis. Additionally, onium chalcogen effects were used to define the mechanism of PchF's methyltransferase reaction.

Materials and Methods

Preparation of full-length PchF (pchf-fl) Overexpression Plasmid.

The *pchF* (Uni-Prot ID O85740) overexpression construct was a gift from the laboratory of Christopher Walsh.[6] The construct received was the kanamycin resistant, pET28b plasmid (Novagen).

Preparation of Overexpression Plasmid containing PchF adenylation, methyltransferase, and thiolation domains (pchf-amt).

The variant plasmid was produced by site directed mutagenesis using Herculase polymerase supplemented with 0-10% DMSO and the genomic DNA from *Pseudomonas aeruginosa* PAO1, which was purified using the DNeasy® Blood & Tissue Kit (Qiagen) as per the manufacturer's instructions. The forward primer (5'-ATT AGA CAT ATG GTC GAG GCG CCG CCG CAG G-3') including an *Nde*I site (underlined) and reverse primer (5'-TA ATA CTC GAG TCA GGT TCC GGC GCG CTG CGC AG-3') including an *Xho*I site (underlined) were used to amplify the gene of interest. The amplified sequence was ligated into the kanamycin resistant pET28b plasmid (Novagen) digested with the same restriction enzymes. Upon sequencing, it was determined that there were an extra 2 nucleotides inserted before the stop codon. Therefore, using QuikChange XL (Agilent), a forward primer (5'-GCA GCG CGC CGG AAT GAC TCG AGC AC-3') and reverse primer (5'-GTC CTC GAG TCA TTC CGG CGC GCT GC-3') were designed to remove the 2-nucleotide insertion before the stop codon (underlined). The isolated plasmid sequence encodes the entire adenylation domain, methyltransferase domain, and thiolation domain, residues 502 to 1483 of PchF-FL.

G667i-pchf-amt Overexpression plasmid.

The variant plasmid was produced by using the kanamycin resistant *pchF-amt* plasmid and the QuikChange XL (Agilent) as per the manufacturer's instructions. The forward primer (5'-GCGGCGGCGGTGATGGCGCCAAGCTC-3') and reverse primer (5'-

GAGCTTGGCGCCATCACCGCCGCCGC-3') were used to mutate the desired nucleotides (underlined). The isolated plasmid was sequenced showing that only the desired mutations were present.

Pa2412 Overexpression Plasmid.

The *pa2412* (Uni-Prot ID Q9I169) overexpression plasmid was a gift from the laboratory of Andrew Gulick.[28] PA2412 is an MbtH-like protein (MLP) that increases *P. aeruginosa* NRPS protein expression including PchF (data not shown).[29–32] The *pa2412* gene is in a modified pET15b plasmid, conferring ampicillin resistance, containing a 5Xhis affinity tag and a TEV protease recognition site in place of the thrombin site[28]

Methanococcus jannaschii (Mj) S-Adenosyl Methionine (AdoMet) Synthetase Overexpression Plasmid was a gift from Doug Markham from the Fox Chase Cancer Institute.[33]

PchF-FL protein overexpression and purification.

BL21 (DE3) *E. coli* containing the *pchf-fl* and *pa2412* expression plasmids were grown in LB broth containing 50 μg/mL kanamycin and 200 μg/mL ampicillin at 37 °C with shaking (250 rpm). Protein expression was induced when the OD_{600} reached ~0.6 by the addition of isopropyl β-D-thiogalactopyranoside (IPTG) to a final concentration of 200 μM. The temperature was reduced to 22 °C following induction. The cells were harvested by centrifugation (4 230 x g, 10 min, 4 °C) after −21 hours. The cell pellet was resuspended in 25 mM Tris-HCl pH 8, 500 mM NaCl, 50 mM imidazole (buffer A). Cells were disrupted by French press (35 000 psi), and cellular debris was removed by centrifugation (23 430 x g, 45 min, 4 °C). The supernatant was applied to a chelating Sepharose fast-flow column (Amersham Biosciences) charged with nickel chloride and pre-equilibrated in buffer A. Two column volumes of buffer A were followed by a 15-column volume linear gradient of 0-500 mM imidazole in buffer A. PchF-FL and PA2412 proteins eluted together in 1 peak at −150 mM imidazole. Fractions containing the proteins of interest were pooled and concentrated using an Amicon stirred cell with YM30. The concentrated fractions were applied to a Superdex 200 size-exclusion column (Amersham Biosciences) equilibrated with 50 mM Tris pH 8, 150 mM sodium citrate, 10% (v/v) glycerol (buffer B). PchF-FL eluted separately from PA2412 and the PchF-FL fractions were concentrated as above to 1.4 mg/mL as determined by the general Beer-Lambert law and the predicted A_{280} of $\varepsilon = 276\,620\ M^{-1}\ cm^{-1}$ (ProtParam)[34] A total of 14.7 mg was obtained from the 2 L of cell growth. The protein was flash cooled and stored at −80 °C.

PchF-AMT and G667I-PchF-AMT protein overexpression and purification.

BL21 (DE3) *E. coli* containing the *pchf-amt or g667i-pchf-amt* and *pa2412* expression plasmids were grown in LB broth containing 50 μg/mL kanamycin and 200 μg/mL ampicillin at 37 °C with shaking (225 rpm). When the OD_{600} reached −0.6, protein expression was induced by the addition of IPTG to a final concentration of 200 μM and the temperature was reduced to 15 °C. The cells were harvested by centrifugation (4 230 x g, 10 min, 4 °C) after −26 hours. The cell pellet was resuspended in 25 mM Tris-HCl pH 8, 500 mM NaCl, 5 mM imidazole, 10 % glycerol (buffer C). Cells were disrupted by use of a

French pressure cell (35 000 psi), and cellular debris was removed by centrifugation (11 950 x g, 60 min, 4 °C). The supernatant was applied to a chelating Sepharose fast-flow column (Amersham Biosciences) charged with nickel chloride and pre-equilibrated in buffer C. After injection, the column was washed with four column volumes of buffer C, followed by four column volumes of 50 mM imidazole in buffer C. A linear gradient from 50-500 mM imidazole in buffer C over six column volumes allowed elution of PchF-AMT or G667I-PchF-AMT and PA2412 proteins in a single peak around 200 mM imidazole. The pooled fractions were dialyzed using SnakeSkin® Dialysis Tubing (10 kDa cutoff) against 50 mM Tris pH 8, 1 mM dithiothreitol (DTT), 10% (v/v) glycerol (buffer D). The dialysate was changed for fresh buffer twice: at 1 and 2 hours before exchanging overnight. The protein solution was loaded onto a Source 30Q (GE Healthcare Life Sciences) anion exchange column pre-equilibrated in buffer D. After injection, two column volumes of buffer D were followed by a 0-500 mM NaCl linear gradient over 15 column volumes in buffer D. PchF-AMT or G667I- PchF-AMT eluted at −150 mM NaCl. The collected fractions were concentrated and applied to a Superdex 200 size-exclusion column (Amersham Biosciences) equilibrated with 50 mM Tris pH 8, 100 mM sodium citrate, 1 mM DTT, 10% (v/v) glycerol (buffer C). The fractions containing PchF-AMT or G667I-PchF-AMT were pooled and concentrated using a 30 kDa cutoff Amicon ultracentrifugal spin filter. The final concentration of PchF-AMT was 7.8 mg/mL as determined by the general Beer-Lambert law and the predicted A_{280} of ε = 149 310 M^{-1} cm^{-1} (ProtParam).[34] A total of 13.3 mg of PchF-AMT was obtained from the 3 L cell growth. The protein was flash cooled and stored at −80 °C. G667I-PchF-AMT was concentrated to 1.4 mg/mL, also determine by Beer-Lambert's law and the predicted A_{280} of ε = 149 310 M^{-1} cm^{-1} (ProtParam).[34] A total of 0.621 mg was obtained from the 3 L cell growth. The protein was flash cooled and stored at −80°C.

Methanococcus jannaschii (Mj) AdoMet Synthetase (Uni-Prot ID Q58605) overexpression and purification.

BL21 (DE3) *E. coli* containing the pMJ 1208-1 expression plasmid were grown in LB broth containing 100 μg/mL ampicillin at 37 °C with shaking (225 rpm). When the OD_{600} reached ~0.6, protein expression was induced by the addition of IPTG to a final concentration of 500 μM. Cultures were incubated for an additional 5 hours. The cells were harvested by centrifugation (10 820 x g, 10 min, 4 °C). The cell paste (50 g) was resuspended in 50mM HEPES pH 7.5, 10 mM β-mercaptoethanol, 300 mM NaCl, 5 mM imidazole, supplemented with 1 mg/mL lysozyme, 0.1 mg/mL DNAse I, 1 mM PMSF, and 0.1% Triton X (Buffer E). Cells were lysed by sonication (6 cycles of 45 seconds with 7 minutes between cycles, 4°C) and subsequently heat denatured (50 min, 75°C). Cell debris and denaturants were removed by centrifugation (50 000 x g, 60 min, 4°C). The supernatant was loaded onto a Ni-NTA agarose column equilibrated with Buffer E. The column was washed with five column volumes of Buffer E and eluted with Buffer E supplemented with 500 mM imidazole. Fractions containing protein were concentrated using a 10 kDa cutoff Amicon ultracentrifugal spin filter. The protein was loaded onto a G-25 column equilibrated in 50 mM Tris-HCl pH 8, 50 mM KCl, 0.1% BME, 10% (v/v) glycerol (Buffer F). Protein containing fractions determined by Bradford assay and were collected and concentrated using a 30-kDa cutoff Amicon ultracentrifugal spin filter. The concentrated protein was

determined by the general Beer-Lambert law and the predicted A_{280} of ε = 24 870 M^{-1} cm^{-1} (ProtParam) before being flash cooled and stored at −80 °C.[34] A total of 211 mg of *Mj* AdoMet synthetase was obtained from the 10 L of cell growth.

Preparation of Substrate Analogues (Scheme 1).

General experimental procedures.—Chemical reagents purchased from commercial suppliers were not further purified prior to use. Flash column chromatography was performed using silica gel (4-63 mm) purchased from Sorbent Technologies. Other chemical separations were performed using a Teledyne Isco CombiFlash Rf. A Biotage microwave reactor was used when microwaving was necessary. ^{1}H and ^{13}C NMR were recorded using a 500 MHz Bruker AVIII spectrometer equipped with a cryogenically-cooled carbon observe probe. Tetramethylsilane was used as an internal standard and chemical shifts (δ) are reported in ppm and coupling constants (*J*) are reported in Hz. High-resolution mass spectrometry (HRMS) was performed using an electrospray ion source in either positive or negative mode on an LCT Premier (Micromass Ltd., Manchester UK). Melting points were measured with a Thomas Capillary Melting Point Apparatus and are uncorrected. Chiral analysis was carried out using HPLC, 1 ml/min hexane:isopropanol (90:10) on a CHIRALCEL® OD-H column, monitored at 320 nm unless otherwise specified.

2-(2-hydroxyphenyl)thiazole-4-carbaldehyde—A microwave vial was charged with 2-bromothiazole-4-carbaldehyde (2.08 mmol), 2-hydroxyphenyl boronic acid (2.71 mmol), and $Pd(PPh_3)_4$ (0.104 mmol). The vial was sealed and flushed with argon for 5 minutes. Dimethoxyethane (16 mL) and a 2 M potassium carbonate solution (2.0 mL, 4.17 mmol) were added through the septum, the reaction was stirred at room temperature for an additional 5 minutes and heated to 100°C for 45 minutes using a microwave reactor. The reaction was cooled to room temperature and filtered through a pad of celite and sepharose. The reaction was concentrated under reduced pressure and purified using flash chromatography (0:1-1:6 EtOAc/Hexane gradient) to yield a yellow solid (300 mg, 70%). The purified product was in agreement with literature values for melting point, ^{1}H NMR, and ^{13}C NMR.[35]

(2RS-4R)-2-(2-(2-hydroxyphenyl)thiazol-4-yl)thiazolidine-4-carboxylic acid ($HPT_{ox}T_{red}$-CO_2^-)>—2-(2-Hydroxyphenyl)thiazole-4-carbaldehyde (1.46 mmol) and potassium acetate (9.71 mmol) were dissolved in a solution of EtOH/L_2O (10:3, 104 mL) in a round bottom flask. L-Cysteine-HC1 (5.40 mmol) was added and the reaction was stirred at room temperature for 1 hour. The reaction was washed with hexanes (50 mL), diluted with H_2O and acidified with citric acid to ~pH 2. The aqueous layer was extracted with CH_2CI_2 (3 × 75 mL). The organic layers were combined and dried over Na_2SC_4. The solvent was removed in vacuo to afford a yellow/white solid (430 mg, 95%). The product was purified as a mixture of epimers and was in agreement with literature values for ^{1}H NMR and ^{13}C NMR.[36] HRMS: $[M + H]^+$ 309.0289 (calcd), 309.0363 (found).

Ethyl (2RS-4R)-2-(2-(2-hydroxyphenyl)thiazol-4-yl)thiazolidine-4-carboxylate ($HPT_{ox}T_{red\text{-}CO_2}ET$).—Thionyl chloride (1.75 mmol) was added dropwise to anhydrous ethanol (3.25 mL) with vigorous stirring in a −10°C ice water bath. The mixture was

warmed to room temperature. $HPT_{ox}T_{red}$-CO_2^{-1} (0.649 mmols) was added and the reaction was heated to 40 °C and stirred for 16 hours. The mixture was cooled to room temperature and the solvent was removed in vacuo. The residue was reconstituted in saturated Na2CC>3 (30 mL) and extracted with CH_2Cl_2 (4 × 50 mL). The organic layers were combined, and the mixture was concentrated under reduced pressure and purified using the CombiFlash (0:1-1:2 EtOAc/Hexane gradient) to yield a clear oil (119 mg, 55%). The product was purified as a diastereomer (38:62) as determined by chiral chromatography (Figure S2). **^{1}H NMR** (500 MHz, DMSO-d_6) δ 11.50 (d, J = 764.2 Hz, 2H), 8.37 (s, 1H), 8.05 (dd, J = 7.9, 1.7 Hz, 1H), 8.02 (dd, J = 7.9, 1.7 Hz, 1H), 7.69 (s, 1H), 7.57 (s, 1H), 7.34–7.21 (m, 2H), 7.00 (ddd, J = 8.3, 5.4, 1.2 Hz, 2H), 6.91 (dddd, J = 8.1, 7.2, 5.7, 1.1 Hz, 2H), 5.84 (d, J = 9.9 Hz, 1H), 5.72 (d, J, 12.1 Hz, 1H), 4.41 (ddd, J = 8.7, 6.9, 5.1 Hz, 1H), 4.25 – 4.10 (m, 4H), 4.03 – (ddd, J = 12.1, 8.8, 7.0 Hz, 1H), 3.94 (t, J = 9.4 Hz, 1H), 3.59 (t, J = 12.2 Hz, 1H), 3.42−3.30 (m, 1H), 3.15 – 3.03 (m, 1H), 1.21 (td, J = 7.1, 4.7 Hz, 6H)**^{13}C NMR** 126 MHz, DMSO-d_6) δ 171.30, 170.84, 164.90, 163.92, 163.59, 155.35, 154.87, 152.37, 131.22 – 131.01 (m), 127.43, 127.34, 119.27, 118.95, 118.82, 116.64, 116.51, 115.14, 67.06, 65.23, 64.96, 61.08, 60.80, 38.03, 37.94, 14.08, 14.04. HRMS: $[M + H]^+$ 337.0675 (calcd), 337.0708 (found).

(S)-2-(2-hydroxyphenyl)-4,5-dihydrothiazole-4-carboxylic acid (HPT-CO_2^-)— Synthesis was performed as previously described in Bergeron *et al* and Zamri *et al* except starting materials differed by using D-cysteine instead of L-cysteine.[37,38] Product analysis agreed with previously reported ^{1}H NMR and ^{13}C NMR. HRMS: $[M + H]^+$ 224.0303 (calcd), 224.0378 (found). Chiral analysis was performed using HPLC and a CHIRALCEL® OD-H column. Elution was performed using a hexane:isopropanol (90:10) mixture supplemented with 0.1% trifluoroacetic acid at a flow rate of 0.500 mL/min, R_f = 14.7 minutes.

Dimethyl 3,3'-disulfanediyl(2R,2'R)-bis(2-((S)-2-(2-hydroxyphenyl)-4,5-dihydrothiazole-4-carboxamido)propanoate)—D-HPT-CO_2^-, L-cystine dimethyl ester dichloride (Sigma), and 1-cyano-2-ethoxy-2-oxoethylidenaminooxy)dimethylamino-morpholino-carbenium hexafluorophosphate (Sigma) were purged under argon in a 25 mL round bottom flask before being dissolved in DMF (10 mL) at 0°C. Diisopropylethylamine was then added dropwise and the reaction was stirred vigorously for 1 hour at 4°C and 3 hours at room temperature. Ethyl acetate (50 mL) was then added to the reaction. The organic fraction was washed with 1M HC1 (2 × 50 mL), water (2 × 50 mL), and brine (2 × 50 mL) before being concentrated under reduced pressure. The residue was purified using the CombiFlash (DCM from 0-5 minutes before a gradient to 5% MeOH from 5-8 minutes and holding the 5% MeOH in DCM for 5 more minutes) eluting a peak at 10 minutes. An additional purification step was performed using a Waters Acquity UPLC with a photodiode array UV detector and an LCT premiere TOF mass spectrometer. The UPCL/HRMS used a gradient elution increasing 20% CH_3CN in water over 5 minutes. Injections of a 1 mL DMSO stock were made onto a Waters (T3 Cl8) 19 × 150 mm, 5 μm column with a flow rate of 20 mL/min to yield a white solid (35 mg, 12%). **^{1}H NMR** (500 MHz, DMSO-d_6) δ 12.09 (s, 1H), 8.86 (d, J = 8.0 Hz, 1H), 7.45 (ddd, J = 15.5, 7.8, 1.7 Hz, 2H), 7.02 – 6.92 (m, 2H), 5.38 (t, J = 9.0 Hz, 1H), 4.68 (td, J = 8.7, 4.8 Hz, 1H), 3.66 (s, 3H), 3.55 (dd, J = 11.1,

8.4 Hz, 1H), 3.23 (dd, J = 13.9, 4.9 Hz, 1H), 3.07 (dd, J = 13.9, 9.1 Hz, 1H). **^{13}C NMR** 126 MHz, DMSO-d_6) δ 173.03, 171.05, 169.83, 158.61, 134.75, 131.09, 119.79, 117.35, 116.24, 77.99, 54.07, 52.32, 33.93. HRMS: $[M + H]^+$ 679.0946 (calcd), 679.1008 (found).

Preparation of Co-substrate Analogues.

Se-Adenosyl selenomethionine (SeAdoMet).—SeAdoMet was biosynthesized and purified by a modification of known methods.[39] 10 mM L-methionine was added to a reaction mixture containing 100 mM Tris pH 8, 50 mM KC1, 40 mM $MgCl_2$, 15 mM ATP, 8% 2-mercaptoethanol, 1.3 U inorganic pyrophosphatase (Sigma), 130 μM *Mj* AdoMet Synthetase in a final volume of 10 mL. The reaction was gently rocked for 4 hours, quenched with 1 mL 1 M H_2SO_4, and neutralized with 1 mL 2.5 M Ammonium Acetate. The mixture was centrifuged (3 082 x g for 10 minutes at 4°C), flash cooled, and stored as 800 μL aliquots at −80°C for further purification. 400 μL was injected onto a Waters Semi-Prep C18 column (10 × 250 mm, 5μM) previously equilibrated in 95% 83 mM triethyl ammonium amine pH 5 (solvent A) and 5% methanol running at 5 mL/min. SeAdoMet was isolated at 3.7 minutes. A linear gradient of 0-50% acetonitrile and 5-50% methanol from 8-18 minutes was used to flush the column. A gradient back to 95% solvent A and 5% methanol was performed at 19 minutes to re-equilibrate the column for subsequent runs. Immediately after collection, SeAdoMet was flash cooled and lyophilized overnight. The lyophilized sample was resuspended in 250 μL of 100 mM H_2SO_4 and the concentration was determined spectrophotometrically (AdoMet, ε_{260} = 15 400 $M^{-1}cm^{-1}$)[40] to be 35.3 mM.

Te-Adenosyl telluromethionine (TeAdoMet).—The TeAdoMet was synthesized as previously described.[39]

Steady-state Adenylation Assay

Reactions contained 50 mM Tris pH 7.5, 1 mM $MgCl_2$, 200 μM 2-amino-6-mercapto-7-methylpurine ribonucleoside (MesGR), 0.002 U purine nucleoside phosphorylase (PNP, Sigma), 0.001 U inorganic pyrophosphatase (IPP, Sigma), 2 mM ATP, 150 mM hydroxylamine, 0.600 μM enzyme, and varying concentrations of L-cysteine. Stock concentrations (200 mM – 12.5 μM) of L-cysteine were prepared by serial dilution in 25 mM Tris pH 8 buffer supplemented with 5 mM dithiothreitol. ATP, L-cysteine, and hydroxylamine were made fresh for each triplicate reaction. A parent mixture containing all reaction components except L-cysteine were incubated for 15 minutes at room temperature. The reaction (final volume, 100μL) was initiated by the addition of the parent mixture to substrate in a 96-well flat bottom plate (Corning Cat. #9017) and production of 2-amino-6-mercapto-7-methylpurine (MesG) was monitored at A_{360} on a Cary 50 UV-VIS Spectrophotometer with a plate reader attachment. Steady-state turnover was converted from *AU/min* to *μM/min* using the general Beer-Lambert law using 0.29 cm as the path-length and 11,000 $cm^{-1}M^{-1}$ as the molar extinction coefficient of MesG.[41] The calculated rate was divided in half because each pyrophosphate released from the adenylation activity undergoes catalytic hydrolysis by inorganic pyrophosphatase creating two inorganic phosphates, both used individually by purine nucleoside phosphorylase to convert MesGR to MesG. Negative controls (without enzyme, without L-cysteine, and without ATP) were carried out with each triplicate reaction. The largest rate from the multiple negative control reactions was

subtracted as background from all of the calculated rates. Triplicate trials were performed twice, on separate days for each enzyme. The initial rates were fit to the Michaelis-Menten equation using the nonlinear regression function of KaleidaGraph (Synergy Software). Kinetic parameters were calculated for each of the six individual trials per enzyme. The reported values represent the average and standard deviation of these six sets of kinetic parameters.

Methyltransferase Activity Assay

Methylated product formation assay.—Methyltransferase activity was observed with $HPT_{ox}T_{red}$-CO_2Et, but not observed with $HPT_{ox}T_{red}$-CO_2^-, $HPT_{ox}T$-CO_2Et,[42] or HPT-Cys-Me at 50 μM during a 1-hour incubation. Product formation of $HPT_{ox}T_{red\text{-}M}$-CO_2Et was monitored at A_{320} by HPLC and confirmed by selected ion recording mass spectrometry. Each assay mixture (100 μL) contained 100 mM Tris-HCl pH 8.0, 45 nM enzyme, 1 mM AdoMet, varying amounts of HPT_{ox}Tred-CO_2Et (1 μM – 30 μM) in DMSO (final DMSO concentration ≤ 2%), and 1 mM tryptophan (an internal standard). A parent mixture of all reaction components, excluding $HPT_{ox}T_{red}$-CO_2Et, was incubated at room temperature for 5 minutes before initiating the reaction with $HPT_{ox}T_{red}$-CO_2Et. A time-course assay was performed for both low (1 μM) and high (30 μM) $HPT_{ox}T_{red}$-CO_2Et to determine that 15 minutes was within the linear steady-state turnover for PchF-FL and PchF-AMT. Therefore, an endpoint assay was employed after a 15-minute incubation at room temperature. Reactions were quenched with 5 μL of 1 M H_2SO_4, vortexed, and neutralized with 10 μL of 1M sodium citrate pH 5.5.

S-adenosylhomocysteine formation assay.—Methyl transferase activity by PchF-AMT or PchF-FL was assessed with the substrates $HPT_{ox}T_{red}$-CO_2Et or L-Cys-OEt (Sigma) by measuring the formation of the coproduct, *S*-adenosyl homocysteine (AdoHCys), following a 3-hour incubation. Each assay mixture (100 μL) contained 100 mM Tris-HCl pH 8.0, 1 μM enzyme (PchF-AMT or PchF-FL), 1 mM AdoMet, and 30 μM $HPT_{ox}T_{red}$-CO_2Et or 30 μM or 3 mM L-Cys-OEt. Reactions were quenched with 5 μL of 1 M H_2SO_4 and neutralized with 10 μL of 1M sodium citrate pH 5.5. A Waters Acquity UPLC was used to inject 10 μL of sample onto a Phenomenex Luna silica C18 column (4.6 X 250 mm, 5 μM) previously equilibrated in 99% solvent B (0.016% formic acid, 0.02% triethylamine) and 1% acetonitrile. Isocratic flow of 99% Solvent B : 1% ACN at 0.8 mL/min for 10 minutes separated AdoMet (3.0 min) and AdoHCys (7.0 min), as measured by absorbance at 260 nm. To determine the concentration of AdoHCys a standard curve was generated by plotting the area of the elution peaks at varied AdoHCys concentrations. Final AdoHCys concentrations are reported in μM after subtracting for AdoHCys formed by non-enzymatic decomposition as measured in negative controls. Measurements were made for at least 3 replicates of all reaction and standard curve trials.

Steady-state kinetics varying onium chalcogen co-substrates using the methylated product formation assay.—Each assay mixture (100 μL) contained 100 mM Tris-HCl pH 8.0, 45 nM enzyme, 50 μM $HPT_{ox}T_{red}$-CO_2Et, varying amounts of AdoMet, SeAdoMet or TeAdoMet (0-2 mM), and 1 mM tryptophan (an internal standard). A parent mixture of all reaction components, excluding AdoMet, SeAdoMet, or TeAdoMet,

was incubated at room temperature for 5 minutes before initiating the reaction with AdoMet, SeAdoMet or TeAdoMet. Reactions were quenched with 5 μL of 1 M H_2SO_4, vortexed, and neutralized with 10 μL of 1 M sodium citrate pH 5.5. Linear steady-state turnover was assessed for low (5 μM) and high (1 mM) concentrations of AdoMet and SeAdoMet. The reaction was quenched at 10 minutes, within the linear steady-state for both AdoMet and SeAdoMet. TeAdoMet reactions, also within steady-state, were incubated for 4 hours and contained twice the concentration of enzyme. AdoMet was varied in reactions from 0 – 2000 μM, SeAdoMet was varied from 0 – 650 μM, whereas TeAdoMet was varied from 0 – 800 μM.

Methyltransferase steady-state kinetic analysis using the methylated product formation assay.—Quenched and neutralized methyltransferase reaction samples were centrifuged (10 600 x g, 10 mins, 4 °C) to remove denatured enzyme, and 100 μL of supernatant was injected onto an IRIS Technologies LLC IProSIL C18 column (4.6 X 250 mm, 5 μM) previously equilibrated in 92% solvent B (0.016% formic acid, 0.02% triethylamine) and 8% acetonitrile. A linear gradient of 8-80% acetonitrile from 0-15 mins, an 80-100% linear gradient from 15-20 minutes, and a 100-8% gradient from 20-21 minutes at 1 mL/min gave good separation of $HPT_{ox}T_{red}$-CO_2Et (19.9 min) and methylated $HPT_{ox}T_{red}$-CO_2Et (21.6 min). A standard curve for product formation was determined by monitoring assay completion of 0-10 μM $HPT_{ox}T_{red}$-CO_2Et reactions with PchF-AMT performed in triplicate (9 000 ±100 mV/μM, Figure S5). Due to substrate concentrations being less than 100 times enzyme concentration, Equation 1 was used to calculate steady-state parameters.[43] The reported kinetic parameters were calculated by finding the average and standard deviation of each individual assay performed in triplicate.

$$v = V_{max}\left(\frac{([E]_t + [S]_t + K_s) - \sqrt{(([E]_t) + ([E]_t) + K_s)^2 - 4([E]_t)([S]_t)}}{2([E]_t)}\right) + m_4 x \quad \text{Equation 1.}$$

Results

Cloning, sequencing, and purification of PchF-FL, PchF-AMT, and G667I-PchF-AMT.

Three variants of PchF were generated heterologously in an *E. coli* expression system. The first is the full-length protein as produced by *P. aeruginosa,* called PchF-FL herein (Figure 1B). The second consists of the adenylation-methyltransferase-didomain with the thiolation domain, and is thus abbreviated PchF-AMT. This construct removes the *N*-terminal cyclization domain and the *C*-terminal thioesterase domain to eliminate confounding activities. Previously, Patel and colleagues developed a pyochelin reconstitution assay using recombinant PchD, PchE, PchF, PchG with substrates and cofactors, monitoring the formation of mature pyochelin by HPLC analysis.[10] Patel *et al* reported that mutation of the second glycine of a core AdoMet binding motif (GxG) to an arginine (G1167R) in PchF resulted in undetectable amounts of pyochelin.[10] The authors suggested that pyochelin formation was inhibited due to a lack of methyl transfer from AdoMet to the $HPTT_{red}$ intermediate (Figure 1B-D). We attempted to generate G667R-PchF-AMT, but overexpression yielded negligible amounts of protein. We therefore proposed that

substitution of the same glycine with a bulky hydrophobic residue would likewise inhibit AdoMet binding, and designed a glycine to isoleucine mutation, G667I-PchF-AMT, which proved easier to purify in necessary amounts for kinetic analysis.

Each of the PchF variants was co-expressed with PA2412, an MbtH-like protein (MLP) from the pyoverdin biosynthetic cluster of *P. aeruginosa,* which increases the amount of the PchF variants purified. This is consistent with other reports that have shown that MLPs greatly enhance NRPS solubility and are sometimes even necessary for expression.[28,29,44,45] Recently, MLPs were co-crystallized with NRPS modules showing complex formation with the adenylation domains.[28, 45-48] While each PchF variant was co-expressed with PA2412 and the proteins co-eluted by nickel chelating chromatography (both are histidine tagged), the proteins were separated by gel filtration chromatography. Therefore, the final purified PchF variants did not contain PA2412. The PchF-AMT and G667I-PchF-AMT purification protocols included an additional anion exchange step to achieve >95% purity, estimated by polyacrylamide gel electrophoresis.

Steady-state kinetics of adenylation activity.

Aldrich *et al* previously described a continuous assay to measure activity of adenylation domains by linking pyrophosphate production to an absorbance change (Figure S3).[49] The coupled assay uses inorganic pyrophosphatase (IPP) to hydrolyze the pyrophosphate generated by the adenylation reaction to two inorganic phosphate ions. Subsequently, purine nucleoside phosphorylase (PNP) converts 7-methylthioguanosine (MesGR) to ribose 1-phosphate and the chromogenic 7-methythioguanine (MesG), with the change measured as an increase in absorbance at 360 nm. This assay was optimized to measure adenylation of L-cysteine in the stuffed adenylation-methyltransferase didomain of PchF-FL, PchF-AMT, and G667I-PchF-AMT. Without hydroxylamine addition, detection of the downstream chromogenic MesG was within error of negative controls through 30 minutes, whereas the inclusion of hydroxylamine gave reliable steady state turnover (Figure 2), suggesting that the adenylation domain remains in a closed conformation and inorganic pyrophosphate is not released until after attachment of the amino acid to the Ppant tether (mimicked here by the hydroxylamine surrogate). A representative assay with and without hydroxylamine can be found in Figure 2, along with Michaelis-Menten curves for the three PchF variants. Steady state kinetic parameters for adenylation of all three constructs can be found in Table 1. Note that k_{cat} values are within 1.2-fold for all three constructs. The K_M values are within 2-fold of each other, which accounts for the similar variance in k_{cat}/K_M. It is interesting to note that adenylation kinetic parameters were found to be an entire magnitude different for PchF-FL than previously reported by Walsh *et al* (Table 1), highlighting discrepancies between the reverse assay measuring the incorporation of radioactive [^{32}P]-pyrophosphate into ATP used by Walsh and the assay described herein. The disparities between these two assays were formerly reported by Aldrich *et al.*[49] It is important to note that all three constructs have similar adenylation parameters, suggesting any differences observed in methyltransferase catalytic efficiency are due to specific changes within the methyltransferase domains.

Substrate analog synthesis.

Kinetic characterization of NRPS domains can be difficult because the biological substrate is attached to the thiolation domain through the Ppant tether. Previously, substrate analogues, the peptidyl *N*-acetylcysteamine thioesters (peptidyl-SNACs), have been synthesized and used to elucidate substrate specificity and kinetic parameters of NRPS domains.[50] For example, Ehmann and colleagues revealed the enantioselectivity of the upstream substrate in the condensation domain of TycB from tyrocidine biosynthesis.[50] Schneider *et al* used peptidyl-SNAC mimics to study the kinetics of the oxidase activity of EpoB from epothilone biosynthesis and BlmIII of bleomycin biosynthesis.[15] Tseng *et al* also generated peptidyl-SNACs, peptidyl *N*-acetylethanolamine esters (ONACs) and peptidyl *N*-acetylethylenediamine amides (NNACs) to probe thioesterase cyclization and hydrolysis capabilities of the thioesterase domain of Srf from surfactin biosynthesis.[51] However, there are several examples where aminoacyl-SNACs or analogs have not been able to replace thiolation domain-bound thioesters or a substrate covalently bonded to CoA, and likely several more examples exist, though have not been published.[52-56] As natural product biosynthesis advances through the NRPS assembly line, intermediates become more complex, often including non-proteogenic amino acids, special tailoring, and enantioselectivity, further complicating organic synthetic routes to generate intermediate analogs.

During reconstitution assays, the growing peptide chain tethered by the phosphopantetheinyl (Ppant) thioester is susceptible to hydrolysis, releasing a carboxylate derivative of the intermediate of the biosynthetic pathway. HPT-Cys-Me, $HPT_{ox}T\text{-}CO_2^-$ and $HPTT_{red}\text{-}CO_2^-$ (Figure 1D) had been detected during pyochelin reconstitution assays.[6,10] As a starting point for synthesis of potential substrate analogs to probe the methyltransferase kinetics of PchF, we generated these compounds, and derivatives altering the carboxyl to a terminal ester generating, HPT-Cys-Me, $HPT_{ox}T\text{-}CO_2Et$ and $HPT_{ox}T_{red}\text{-}CO_2Et$, to mimic the natural thioester linkage of the Ppant tether.

Synthesis of $HPT_{ox}T\text{-}CO_2^-$ and $HPT_{ox}T\text{-}CO_2Et$ was previously reported.[42] For $HPT_{ox}T_{red}\text{-}CO_2^-$ and $HPT_{ox}T_{red}\text{-}CO_2Et$, 2-hydroxyphenyl boronic acid and 2-bromothiazole-4-carbaldehyde were coupled by a Suzuki reaction to generate the 2-(2-hydroxyphenyl)thiazole-4-carbaldehyde product providing a 70% yield (Scheme 1). Condensation of the aldehyde with L-cysteine furnished the desired $HPT_{ox}T_{red}\text{-}CO_2^-$ substrate analog as a diastereomer in 95% yield. The terminal carboxylic acid was transformed to an ethyl ester by generation of an acyl chloride before nucleophilic addition of the solvent ethanol providing $HPT_{ox}T_{red}\text{-}CO_2Et$ in 55% yield also as a diastereomer (Figure S2). HPT-Cys-Me was furnished by first synthesizing D-$HPT\text{-}CO_2^-$ before performing an amino acid coupling with L-cystine using COMU as the coupling reagent. Generation of the free thiol HPT-Cys-Me, was performed *in vitro* by TCEP reduction and was confirmed by LC-HRMS.

Methyltransferase activity.

Using the synthesized substrate analogs, the steady-state capabilities of the stuffed methyltransferase domain of PchF-FL, PchF-AMT, and G667I-PchF-AMT were analyzed

by a discontinuous assay measuring formation of the methylated product in the presence of excess AdoMet. Neither HPT-Cys-Me, $HPT_{ox}T$-CO_2Et, nor $HPT_{ox}T_{red}$-CO_2^- demonstrated methyl transfer after 1-hour incubation. Methylation of $HPT_{ox}T_{red}$-CO_2Et by both PchF-FL and PchF-AMT was observed, generating $HPT_{ox}T_{red\text{-}M}$-CO_2Et, and the substrate and product were separated by HPLC (Figure 3). Product formation was confirmed by secondary ion mass spectrometry. G667I-PchF-AMT did not catalyze methyltransferase activity, even after extending the assay to 10 hours. Kinetic parameters from the methylated product formation assay can be found in Table 2 and Michaelis-Menten plots can be seen in Figure S4. It is important to note that PchF-FL and PchF-AMT provided comparable kinetic parameters using $HPT_{ox}T_{red}$-CO_2Et as a substrate analog, indicating that the three-domain fragment is a viable substitute for the full-length protein. The k_{cat} was 1.5-fold greater and the K_M was 2.1-fold greater for PchF-AMT than that of PchF-FL. This resulted in PchF-AMT having a 1.4-fold lower catalytic efficiency compared to PchF-FL. An orthogonal methyltransferase activity assay was developed to determine if the enzymes are capable of methylating L-Cys-OEt. The assay is a three-hour endpoint assay measuring the formation of the coproduct, AdoHCys, separating the reaction components by UPLC and measuring absorbance at 260 nm (Figure S6). $HPT_{ox}T_{red}$-CO_2Et was used as a positive control. PchF-FL generated 25 ± 6 μM AdoHCys and PchF-AMT generated 33 ± 3 μM AdoHCys, within error of equimolar turnover (30 μM $HPT_{ox}T_{red}$-CO_2Et) at the three-hour incubation. Importantly, the quantitation of AdoHCys was within error of negative controls with L-Cys-OEt as a substrate at 3 mM, two orders of magnitude greater than the $HPT_{ox}T_{red}$-CO_2Et concentration, indicating that L-Cys-OEt is not a substrate analog of PchF methylation (Figure 4).

Onium chalcogen effects on the methyltransferase kinetic parameters of PchF variants.

Replacement of the sulfonium of AdoMet with selenonium (SeAdoMet) and telluronium (TeAdoMet) has been used to investigate the mechanism of cyclopropane fatty acid (CFA) synthase. Because the mechanism has been well-defined experimentally, steady-state kinetics of catechol *O*-methyltransferase (COMT) using AdoMet, SeAdoMet, and TeAdoMet were determined and kinetic parameters were used as a control.[57] The primary (k_{cat}) and secondary (k_{cat}/K_M) rate constants for methyltransferase activity of CFA synthase and COMT follow the trend SeAdoMet > AdoMet > TeAdoMet, parallel to the electrophilicities determined for the onium chalcogen.[39,57] Additional kinetic isotope effects (KIEs) using *S*-adenosyl-L-[*methyl-d*$_3$]methionine have been interpreted to support a tight S_N2 transition state for CFA and COMT. The methyltransferase assay described above was performed with varying concentrations of AdoMet and co-substrate analogs, SeAdoMet and TeAdoMet, while keeping $HPT_{ox}T_{red}$-CO_2Et in excess. The effect of AdoMet, SeAdoMet, and TeAdoMet on PchF-FL, PchF-AMT, and G667I-PchF-AMT is displayed in Table 3 and kinetic ratios are reported in Table 4. Michaelis-Menten curves are in Figure S4. When AdoMet was used as the co-substrate for PchF-FL k_{cat} and K_M were 1.2 ± 0.1 min^{-1} and 3.3 ± 0.8 μM. SeAdoMet acted as a better co-substrate displaying a turnover number 1.9-fold greater and the K_M was within error compared to AdoMet.. Substitution of AdoMet with TeAdoMet required the assay to be run 36-times longer (6 hours) with twice the enzyme concentration for both PchF-FL and PchF-AMT to detect product formation. Comparatively, TeAdoMet demonstrated a k_{cat} that was 21-fold slower and a K_M that was 47-fold greater in

comparison to AdoMet. When performing the same assay with PchF-AMT, the kinetic values were comparable, yielding k_{cat}/K_m values within error to those for the full-length protein. Overall, the primary and secondary rate constants for the different onium chalcogen co-substrate and analogs follow the trend for an $_{sN}2$ mechanism.

Discussion

Peptides generated by nonribosomal peptide synthetases are not simply peptides, but have been modified by tailoring domains to provide these natural products with their structural diversity and unique bioactive properties. Tailoring domains can be divided into three categories: independent, stand-alone, and stuffed. Independent tailoring domains are commonly incorporated into NRPS modules following the thiolation domain, modifying the nascent chain *in cis.* Stand-alone tailoring domains, like PchG of pyochelin biosynthesis, are separate enzymes that modify the natural product biosynthetic intermediates *in trans.* Intriguingly, an increasing number of tailoring domains have been identified that are stuffed within the NRPS adenylation domain, replacing loops between signature adenylation domain sequences. [12,13] Natural products built using stuffed tailoring domains have been isolated and used in the clinic as anticancer, antifungal, or antibiotic drugs. However, investigation of stuffed tailoring domains has been limited, leaving the structural and biochemical characterization of these domains and their distinctive integration into the NRPS bioassembly as an emerging area of study.

A mechanistic and structural characterization of the stuffed methyltransferase domains involved in thiocoraline and kutzneride biosynthesis, microbial depsipeptides, has been previously reported.[12, 19, 25-27] These stuffed methyltransferase domains perform *O*-methylation of a serine residue (kutzeride) and *N*- and *S*-methylation of cysteine residues (thiocoraline). An adenylation domain consists of two subdomains, an A_{core} subdomain, which includes the catalytic machinery, and the A_{sub} subdomain that works with the thiolation domain to orient the substrate attached to the Ppant tether into each active site of the NRPS module.[46, 58,59] The methyltransferase domain of the adenylation-methyltransferase didomain of the kutzneride assembly line for *O*-methylation of serine is in the second module of the protein KtzH and is stuffed into a loop of the A_{sub} subdomain between the A8 and A9 adenylation core sequence motifs.[27] The methyltransferase domains of the adenylation-methyltransferase didomains of the thiocoraline assembly line for *N*-methylation are found in the two modules of TioS and are likewise stuffed into loops of the A_{sub} subdomain between the A8 and A9 adenylation core sequence motifs. The didomain for *S*-methylation is in the standalone protein TioN, and the methyltransferase domain is stuffed into loops of the A_{core} subdomain between the A2 and A3 adenylation sequence motifs.[19, 25, 26] The premise of the previous mechanistic work on these didomains was that methylation could occur on the free amino acid, the aminoacyl-AMP intermediate, the amino acid after thiolation (attachment to the Ppant tether), or as part of the condensed chain before being passed to the next module.[19, 25-27] Experiment has ruled out methylation of free serine or cysteine by these didomains.[19, 25-27] The authors maintain that the substrate of the methyltransferase domain is either the aminoacyl-AMP intermediate, or the amino acid after thiolation but before condensation with the growing peptide chain.[19, 25-27]

The first structure of a stuffed adenylation domain from the second module of TioS, co-crystallized with the MbtH-like protein (MLP), TioT, was recently reported to 2.90 Å.[26] The authors describe the structure as a dumbbell with the *N*-terminal A_{core} and methyltransferase domains being the two balls of the dumbbell, with the discontinuous Asub domain connecting these two domains as the dumbbell bar. By comparison to the structures for the initiation module involved in biosynthesis of the antibiotic gramicidin (LgrA) and to the termination module of the enterobactin biosynthetic pathway (EntF), this new structure is in the "thiolation" Conformation[13,46,60]. In other words, the *C*-terminal A_{sub} domain is in position for thiolation chemistry by the adenylation A_{core} subdomain (the conformation for attachment of the amino acid substrate to the Ppant tether), even though the thiolation domain is not present in the TioS construct. The structure is quite valuable, showing for the first time an A_{sub} subdomain interrupted by a tailoring domain and yet maintaining the expected secondary and tertiary structure. [26] However, it does not answer mechanistic questions such as the order of events for peptide formation and tailoring; for example, whether methylation occurs before or after condensation to the nascent peptide.

Adenylation domains are considered the 'gate-keepers' of the growing chain,[61] selective for the amino acid that gets attached to the thiolation domain, and in the case of adenylation-methyltransferase stuffed didomains, successively methylated. If the amino acid attached to the Ppant tether is the substrate for the tailoring domain, then the methylated amino acid could subsequently condense with the upstream growing peptidyl chain. Conversely, the substrate for the stuffed methyltransferase domain could be the condensed product of the module, a last step before interaction with the downstream module. Thiocoraline and kutzneride are complex natural products, and probing the methyltransferase activities that occur late in the biosynthesis becomes increasingly difficult as intermediates become increasingly complex. Thus, studying the stuffed methyltransferase didomain of PchF, also interrupting the A8 and A9 core motifs in the Asub of the adenylation domain, is ideal: pyochelin is a much simpler natural product and intermediate analogs can be easily synthesized.

Previous studies of PchF and pyochelin biosynthesis do not support the model proposed for thiocoraline or kutzneride biosynthesis in which the stuffed methyltransferase didomains act upon the amino acid tethered to the thiolation domain prior to condensation with the upstream peptidyl chain. From reconstitution assays Walsh and colleagues isolated and characterized HPT-Cys-Me, $HPT_{ox}T\text{-}CO_2^-$, and $HPTT_{red}\text{-}CO_2^-$, but not their methylated analogues (Figure 1D). The authors argued that these data indicate that condensation to the upstream nascent peptide, cyclization and reduction all occur before methylation (Figure 1C-D)[6,10,11] However, these data represent a negative result (no methylation was detected in the hydrolyzed intermediates). An orthogonal assay was performed: radioactivity in the methylated, protein-bound product was measured after protein precipitation. The results were acknowledged by the authors to be problematic, but were interpreted to indicate that methylation was the final tailoring step in the biosynthesis.[10]

Methylation may occur prior to condensation, after condensation and before cyclization, after cyclization and before reduction, or after cyclization and reduction directly prior to release of the mature peptide (Figure S1).[6,10,11] To decipher when on the pathway

methylation occurs, intermediate analogs were synthesized mimicking isolates from the reconstitution assays (Figure 1D): L-Cys-OEt is an ester analog after thiolation of the amino acid to the Ppant tether; HPT-Cys-Me is an ester analog mimicking the growing peptide chain after condensation and before cyclization; $HPT_{ox}T$-CO_2Et is an ethyl ester mimicking the growing peptide chain after cyclization but before reduction; and $HPT_{ox}T_{red}$-CO_2Et mimics the growing chain after cyclization and reduction. Importantly, methyl transfer was only observed when $HPT_{ox}T_{red}$-CO_2Et was used as the substrate analog, indicating that thiolation, condensation, cyclization, and reduction by PchG are necessary events prior to methylation by PchF. It should also be noted that methyl transfer was not observed for the carboxylic acid analogue, $HPT_{ox}T_{red}$-CO_2^-, suggesting that the previously isolated acid is not a substrate. The ester, $HPT_{ox}T_{red}$-CO_2Et, which more closely resembles the natural thioester, serves as a substrate analogue for methyl transfer. Furthermore, an assay measuring formation of the coproduct, AdoHCys, recapitulated that $HPT_{ox}T_{red}$-CO_2Et is a substrate, whereas the ethylester of L-cysteine is not.

Steady-state kinetic parameters were measured for PchF-FL, PchF-AMT, and G667I-PchF-AMT, for both the adenylation and methyltransferase activity. The adenylation activity assay showed that all three constructs, PchF-FL, PchF-AMT, and G667I-PchF-AMT, had similar adenylation parameters, indicating that the methyltransferase variant did not negatively impact the larger didomain (Table 1). While the catalytic efficiency was an order of magnitude less than that previously reported, the assays are significantly different, as documented in the Results section, and similar differences are well documented.[49, 62] A newly defined, discontinuous HPLC methyltransferase assay measuring formation of the methylated product gave reliable kinetic parameters, with the G667I-PchF-AMT variant showing complete loss of methyltransferase activity. While steady state kinetics could be measured for both adenylation and methyltransferase activities, a steady state is not possible in the full thiotemplate production of pyochelin, which is essentially a series of single turnover reactions in a biosynthetic assembly line. Nevertheless, these parameters are useful for testing mechanistic hypotheses.

In 1976, Schowen and colleagues proposed that catechol O-methyltransferase (COMT) used a symmetrical and “tight” S_N2 transition state, one in which the bonds being formed and broken were both short, based on kinetic isotope effects measured with deuterated and ^{13}C-labeled AdoMet.[63] More recently (2016), Luo and colleagues have used similar experiments to probe the transition state of SET8, a lysine methyltransferase, and showed a “tight” yet early asymmetrical transition state, with a *C-N* distance of ~2.4 A and a *C-S* distance of ~2.0 Å.[63, 64] In addition to measuring KIEs and BIEs, the authors also measured steady state kinetic parameters with SeAdoMet and found the values to be in agreement with the slightly weaker *Se-C* bond expected for the leaving group due to the intrinsic chemical properties of the chalcogen.[39] Indeed, onium chalcogen effects have been used to probe methyltransferase activity. By monitoring the formation of 5’-methylthioadenosine (MTA), 5’-methylselenoadenosine (SeMTA), and 5’-methyltelluroadenosine (TeMTA), a model for relative electrophilicities was observed and followed the trend: SeAdoMet > AdoMet > TeAdoMet.[39] Interestingly, substitution of AdoMet with its onium chalcogen analogs used in steady-state analysis with cyclopropane fatty acid synthase and COMT resulted in primary (k_{cat}) and secondary (k_{cat}/K_M) rate constants following the same trend.[57] In this study,

AdoMet and its onium congeners, SeAdoMet and TeAdoMet, were used as co-substrate and co-substrate analogs in the PchF methyltransferase assay. PchF-FL and PchF-AMT exhibited primary and secondary rate constants that followed the SeAdoMet > AdoMet > TeAdoMet trend. By comparison of onium chalcogen steady state kinetics for methyltransferases of determined transition state (Table 4), these results allow us to hypothesize that PchF methyl transfer proceeds by an S_N2 reaction mechanism for this secondary amine.

Conclusion

In summary, we have characterized the stuffed methyltransferase didomain of PchF in pyochelin biosynthesis. Potential substrate analogs were synthesized based on previously recovered biosynthesis intermediates. The stuffed methyltransferase didomain of PchF catalyzes AdoMet dependent methyl transfer, the penultimate step in pyochelin biosynthesis, after thiolation of L-cysteine to the Ppant tether, condensation of the cysteine onto the upstream peptide, cyclization to form the thiazoline, and reduction to form the thiazolidine, but before release of the mature peptide. Onium chalcogen effects suggest that the stuffed methyltransferase domain proceeds through an S_N2 mechanism.

Supplementary Material

Refer to Web version on PubMed Central for supplementary material.

Acknowledgements

Research reported in this publication was made possible by funds from The National Science Foundation (CHE-1403293 to ALL), The National Institute of General Medical Sciences of The National Institutes of Health (P20 GM103418 and R01 GM127655 to ALL, P20 GM113117 to TEP and GM-122595 to SJB). TAR and JSM were supported by the National Institutes of Health Graduate Training Program in the Dynamic Aspects of Chemical Biology (T32 GM008545). JSM was supported by an American Heart Association Predoctoral Fellowship (PRE33960374). Special thanks to KM Meneely, AS Chilton, B Neuenswander, AM Sherwood, EL Onderko, ND Lanz, and MI Radle for technical assistance and support and to N Kenjic for critically reading the manuscript.

Abbreviations

AdoMet	*S*-adenosylmethionine
AdoHCys	*S*-adenosylhomocysteine
CFA	cyclopropane fatty acid synthase
COMT	Catechol *O*-methyltransferase
Cys	cysteine
HP	hydroxyphenyl
HRMS	high-resolution mass spectrometry
IPTG	isopropyl β-D-thiogalactopyranoside

KIEs	kinetic isotope effects
IPP	inorganic pyrophosphatase
MesG	2-amino-6-mercapto-7-methylpurine
MesGR	2-amino-6-mercapto-7-methylpurine ribonucleoside
Mj	*Methanococcus jannaschii*
MLP	MbtH-like protein
MTA	5’-methylthioadenosine
NNACs	*N*-acetylethylenediamine amides
NRPS	nonribosomal peptide synthetase
ONACs	*N*-acetylethanolamine esters
PchF	nonribosomal peptide synthetase from *P. aeruginosa* for the production of pyochelin
PchF-AMT	PchF construct consisting of stuffed adenylation methyltransferase didomains and thiolation domain, and without the condensation and thioesterase domains
PchF-FL	full-length construct of PchF
PNP	purine nucleoside phosphorylase
Ppant	4’phosphopantetheinyl
SeAdoMet	Se-Adenosyl selenomethionine
SeMTA	5’-methylselenoadenosine
SNACs	*N*-acetylcysteamine thioester
T	thiazoline
T_{ox}	thiazole
T_{red}	thiazolidine
$T_{red\text{-}M}$	*N*-methylated thiazolidine
TeAdoMet	Te-Adenosyl telluromethionine
TeMTA	5’-methyltelluroadenosine

References:

[1]. Miethke M, and Marahiel MA (2007) Siderophore-based iron acquisition and pathogen control, Microbiol Mol Biol Rev 71, 413–451. [PubMed: 17804665]

[2]. Cox CD, Rinehart KL, Moore ML Carter Cook J, Jr. (1981) Pyochelin: Novel structure of an iron-chelating growth promoter for Pseudomonas aeruginosa, Proc Natl Acad Sci USA 78, 4256–4260 [PubMed: 6794030]

[3]. Church D, Elsayed S, Reid O, Winston B, and Lindsay R (2006) Burn wound infections, Clin Microbiol Rev 19, 403–434. [PubMed: 16614255]

[4]. Bhagirath AY, Li Y, Somayajula D, Dadashi M, Badr S, and Duan K (2016) Cystic fibrosis lung environment and Pseudomonas aeruginosa infection, BMC Pulm Med 16, 174. [PubMed: 27919253]

[5]. Sadikot RT, Blackwell TS, Christman JW, and Prince AS (2005) Pathogen-host interactions in Pseudomonas aeruginosa pneumonia, Am J Respir Crit Care Med 171, 1209–1223. [PubMed: 15695491]

[6]. Quadri LE, Keating TA, Patel HM, and Walsh CT (1999) Assembly of the Pseudomonas aeruginosa nonribosomal peptide siderophore pyochelin: In vitro reconstitution of aryl-4, 2-bisthiazoline synthetase activity from PchD, PchE, and PchF, Biochemistry 38, 14941–14954. [PubMed: 10555976]

[7]. Reimmann C, Serino L, Beyeler M, and Haas D (1998) Dihydroaeruginoic acid synthetase and pyochelin synthetase, products of the pchEF genes, are induced by extracellular pyochelin in Pseudomonas aeruginosa, Microbiology 144 (Pt 11), 3135–3148. [PubMed: 9846750]

[8]. Serino L, Reimmann C, Visca P, Beyeler M, Chiesa VD, and Haas D (1997) Biosynthesis of pyochelin and dihydroaeruginoic acid requires the iron-regulated pchDCBA operon in Pseudomonas aeruginosa, J Bacteriol 179, 248–257. [PubMed: 8982005]

[9]. Patel HM, Tao J, and Walsh CT (2003) Epimerization of an L-cysteinyl to a D-cysteinyl residue during thiazoline ring formation in siderophore chain elongation by pyochelin synthetase from Pseudomonas aeruginosa, Biochemistry 42, 10514–10527. [PubMed: 12950179]

[10]. Patel HM, and Walsh CT (2001) In vitro reconstitution of the Pseudomonas aeruginosa nonribosomal peptide synthesis of pyochelin: characterization of backbone tailoring thiazoline reductase and N-methyltransferase activities, Biochemistry 40, 9023–9031. [PubMed: 11467965]

[11]. Reimmann C, Patel HM, Serino L, Barone M, Walsh CT, and Haas D (2001) Essential PchG-dependent reduction in pyochelin biosynthesis of Pseudomonas aeruginosa, J Bacteriol 183, 813–820. [PubMed: 11208777]

[12]. Labby KJ, Watsula SG, and Garneau-Tsodikova S (2015) Interrupted adenylation domains: unique bifunctional enzymes involved in nonribosomal peptide biosynthesis, Nat Prod Rep 32, 641–653. [PubMed: 25622971]

[13]. Ronnebaum TA, and Lamb AL (2018) Nonribosomal peptides for iron acquisition: pyochelin biosynthesis as a case study, Curr Opin Struct Biol 53, 1–11. [PubMed: 29455106]

[14]. Schneider TL, and Walsh CT (2004) Portability of oxidase domains in nonribosomal peptide synthetase modules, Biochemistry 43, 15946–15955. [PubMed: 15595851]

[15]. Schneider TL, Shen B, and Walsh CT (2003) Oxidase domains in epothilone and bleomycin biosynthesis: thiazoline to thiazole oxidation during chain elongation, Biochemistry 42, 9722–9730. [PubMed: 12911314]

[16]. Perlova O, Fu J, Kuhlmann S, Krug D, Stewart AF, Zhang Y, and Muller R (2006) Reconstitution of the myxothiazol biosynthetic gene cluster by Red/ET recombination and heterologous expression in Myxococcus xanthus, Appl Environ Microbiol 72, 7485–7494. [PubMed: 16997979]

[17]. Buntin K, Irschik H, Weissman KJ, Luxenburger E, Blocker H, and Muller R (2010) Biosynthesis of thuggacins in myxobacteria: comparative cluster analysis reveals basis for natural product structural diversity, Chem Biol 17, 342–356. [PubMed: 20416506]

[18]. Sattely ES, Fischbach MA, and Walsh CT (2008) Total biosynthesis: in vitro reconstitution of polyketide and nonribosomal peptide pathways, Nat. Prod. Rep 25, 757–793. [PubMed: 18663394]

[19]. Al-Mestarihi AH, Villamizar G, Fernandez J, Zolova OE, Lombo F, and Garneau-Tsodikova S (2014) Adenylation and S-methylation of cysteine by the bifunctional enzyme TioN in thiocoraline biosynthesis, J Am Chem Soc 136, 17350–17354. [PubMed: 25409494]

[20]. De Crecy-Lagard V, Marliere P, and Saurin W (1995) Multienzymatic non ribosomal peptide biosynthesis: identification of the functional domains catalysing peptide elongation and epimerisation, C. R. Acad. Sci. III318, 927–936. [PubMed: 8521076]

[21]. Watanabe K, Hotta K, Praseuth AP, Koketsu K, Migita A, Boddy CN, Wang CC, Oguri H, and Oikawa H (2006) Total biosynthesis of antitumor nonribosomal peptides in Escherichia coli, Nat Chem Biol 2, 423–428. [PubMed: 16799553]

[22]. Sussmuth R, Muller J, von Dohren H, and Molnar I (2011) Fungal cyclooligomer depsipeptides: from classical biochemistry to combinatorial biosynthesis, Nat. Prod. Rep. 28, 99–124. [PubMed: 20959929]

[23]. Kreutzer MF, Kage H, Gebhardt P, Wackier B, Saluz HP, Hoffmeister D, and Nett M (2011) Biosynthesis of a complex yersiniabactin-like natural product via the mic locus in phytopathogen Ralstonia solanacearum, Appl Environ Microbiol 77, 6117–6124. [PubMed: 21724891]

[24]. Christiansen G, Fastner J, Erhard M, Borner T, and Dittmann E (2003) Microcystin biosynthesis in planktothrix: genes, evolution, and manipulation, J. Bacteriol. 185, 564–572. [PubMed: 12511503]

[25]. Mori S, Garzan A, Tsodikov OV, and Garneau-Tsodikova S (2017) Deciphering Nature's Intricate Way of N,S-Dimethylating l-Cysteine: Sequential Action of Two Bifunctional Adenylation Domains, Biochemistry 56, 6087–6097. [PubMed: 29112395]

[26]. Mori S, Pang AH, Lundy TA, Garzan A, Tsodikov OV, and Garneau-Tsodikova S (2018) Structural basis for backbone N-methylation by an interrupted adenylation domain, Nat Chem Biol 14, 428–430. [PubMed: 29556104]

[27]. Zolova OE, and Garneau-Tsodikova S (2014) KtzJ-dependent serine activation and O-methylation by KtzH for kutznerides biosynthesis, J Antibiot (Tokyo) 67, 59–64. [PubMed: 24105608]

[28]. Drake EJ, Cao J, Qu J, Shah MB, Straubinger RM, and Gulick AM (2007) The 1.8 A crystal structure of PA2412, an MbtH-like protein from the pyoverdine cluster of Pseudomonas aeruginosa, J Biol Chem 282, 20425–20434. [PubMed: 17502378]

[29]. Boll B, Taubitz T, and Heide L (2011) Role of MbtH-like proteins in the adenylation of tyrosine during aminocoumarin and vancomycin biosynthesis, J Biol Chem 286, 36281–36290. [PubMed: 21890635]

[30]. Felnagle EA, Barkei JJ, Park H, Podevels AM, McMahon MD, Drott DW, and Thomas MG (2010) MbtH-like proteins as integral components of bacterial nonribosomal peptide synthetases, Biochemistry 49, 8815–8817. [PubMed: 20845982]

[31]. Ochsner UA, Wilderman PJ, Vasil AI, and Vasil ML (2002) GeneChip expression analysis of the iron starvation response in Pseudomonas aeruginosa: identification of novel pyoverdine biosynthesis genes, Mol Microbiol 45, 1277–1287. [PubMed: 12207696]

[32]. Zhang W, Heemstra JR, Jr., Walsh CT, and Imker HJ (2010) Activation of the pacidamycin PacL adenylation domain by MbtH-like proteins, Biochemistry 49, 9946–9947. [PubMed: 20964365]

[33]. Lu ZJ, and Markham GD (2002) Enzymatic properties of S-adenosylmethionine synthetase from the archaeon Methanococcus jannaschii, J Biol Chem 277, 16624–16631. [PubMed: 11872742]

[34]. Gasteiger E, Hoogland C, Gattiker A, Duvaud S, Wilkins MR, Appel RD, Bairoch A (2005) Protein Identification and Analysis Tools on the ExPASy Server, Walker John M. *(ed):* The Proteomics Protocols Handbook, Humana Press, 571–607

[35]. Cuppels DA, Stipanovic RD, Stoessl A, and Stothers JB (1987) C-13mr Studies .132. The Constitution and Properties of a Pyochelin Zinc Complex, Canadian Journal of Chemistry-Revue Canadienne De Chimie 65, 2126–2130.

[36]. Mislin GL, Burger A, and Abdallah MA (2004) Synthesis of new thiazole analogues of pyochelin, a siderophore of Pseudomonas aeruginosa and Burkholderia cepacia. A new conversion of thiazolines into thiazoles, Tetrahedron 60, 12139–12145.

[37]. Zamri A, and Abdallah MA (2000) An improved stereocontrolled synthesis of pyochelin, siderophore of *Pseudomonas aeruginosa* and *Burkholderia cepacia*, Tetrahedron 56, 249–256.

[38]. Bergeron RJ, Wiegand J, Dionis JB, Egli-Karmakka M, Frei J, Huxley-Tencer A, and Peter HH (1991) Evaluation of desferrithiocin and its synthetic analogues as orally effective iron chelators, J Med Chem 34, 2072–2078. [PubMed: 2066978]

[39]. Iwig DF, and Booker SJ (2004) Insight into the polar reactivity of the onium chalcogen analogues of S-adenosyl-L-methionine, Biochemistry 43, 13496–13509. [PubMed: 15491157]

[40]. Schlenk F, and Depalma RE (1957) The formation of S-adenosylmethionine in yeast, J Biol Chem 229, 1037–1050. [PubMed: 13502363]

[41]. Webb MR (1992) A continuous spectrophotometric assay for inorganic phosphate and for measuring phosphate release kinetics in biological systems, Proc Natl Acad Sci U S A 89, 4884–4887. [PubMed: 1534409]

[42]. Meneely KM, Ronnebaum TA, Riley AP, Prisinzano TE, and Lamb AL (2016) Holo Structure and Steady State Kinetics of the Thiazolinyl Imine Reductases for Siderophore Biosynthesis, Biochemistry 55, 5423–5433. [PubMed: 27601130]

[43]. Segel IH (1975) Enzyme kinetics : behavior and analysis of rapid equilibrium and steady state enzyme systems, Wiley, New York.

[44]. Heemstra JR, Jr., Walsh CT, and Sattely ES (2009) Enzymatic tailoring of ornithine in the biosynthesis of the Rhizobium cyclic trihydroxamate siderophore vicibactin, J Am Chem Soc 131, 15317–15329. [PubMed: 19778043]

[45]. Miller BR, Drake EJ, Shi C, Aldrich CC, and Gulick AM (2016) Structures of a Nonribosomal Peptide Synthetase Module Bound to MbtH-like Proteins Support a Highly Dynamic Domain Architecture, J Biol Chem 291, 22559–22571. [PubMed: 27597544]

[46]. Drake EJ, Miller BR, Shi C, Tarrasch JT, Sundlov JA, Allen CL, Skiniotis G, Aldrich CC, and Gulick AM (2016) Structures of two distinct conformations of holo-non-ribosomal peptide synthetases, Nature 529, 235–238. [PubMed: 26762461]

[47]. Herbst DA, Boll B, Zocher G, Stehle T, and Heide L (2013) Structural basis of the interaction of MbtH-like proteins, putative regulators of nonribosomal peptide biosynthesis, with adenylating enzymes, J Biol Chem 288, 1991–2003. [PubMed: 23192349]

[48]. Tarry MJ, Haque AS, Bui KH, and Schmeing TM (2017) X-Ray Crystallography and Electron Microscopy of Cross- and Multi-Module Nonribosomal Peptide Synthetase Proteins Reveal a Flexible Architecture, Structure 25, 783>–793 e784. [PubMed: 28434915]

[49]. Wilson DJ, and Aldrich CC (2010) A continuous kinetic assay for adenylation enzyme activity and inhibition, Anal Biochem 404, 56–63. [PubMed: 20450872]

[50]. Ehmann DE, Trauger JW, Stachelhaus T, and Walsh CT (2000) Aminoacyl-SNACs as small-molecule substrates for the condensation domains of nonribosomal peptide synthetases, Chem Biol 7, 765–772. [PubMed: 11033080]

[51]. Tseng CC, Bruner SD, Kohli RM, Marahiel MA, Walsh CT, and Sieber SA (2002) Characterization of the surfactin synthetase C-terminal thioesterase domain as a cyclic depsipeptide synthase, Biochemistry 41, 13350–13359. [PubMed: 12416979]

[52]. Piasecki SK, Taylor CA, Detelich JF, Liu J, Zheng J, Komsoukaniants A, Siegel DR, and Keatinge-Clay AT (2011) Employing modular polyketide synthase ketoreductases as biocatalysts in the preparative chemoenzymatic syntheses of diketide chiral building blocks, Chem Biol 18, 1331–1340. [PubMed: 22035802]

[53]. Haynes SW, Ames BD, Gao X, Tang Y, and Walsh CT (2011) Unraveling terminal C-domain-mediated condensation in fungal biosynthesis of imidazoindolone metabolites, Biochemistry 50, 5668–5679. [PubMed: 21591693]

[54]. Franke J, and Hertweck C (2016) Biomimetic Thioesters as Probes for Enzymatic Assembly Lines: Synthesis, Applications, and Challenges, Cell Chem Biol 23, 1179–1192. [PubMed: 27693058]

[55]. Foulke-Abel J, and Townsend CA (2012) Demonstration of starter unit interprotein transfer from a fatty acid synthase to a multidomain, nonreducing polyketide synthase, Chembiochem 13, 1880–1884. [PubMed: 22807303]

[56]. Hiratsuka T, Suzuki H, Kariya R, Seo T, Minami A, and Oikawa H (2014) Biosynthesis of the structurally unique polycyclopropanated polyketide-nucleoside hybrid jawsamycin (FR-900848), Angew Chem Int Ed Engl 53, 5423–5426. [PubMed: 24756819]

[57]. Iwig DF, Grippe AT, McIntyre TA, and Booker SJ (2004) Isotope and elemental effects indicate a rate-limiting methyl transfer as the initial step in the reaction catalyzed by Escherichia coli cyclopropane fatty acid synthase, Biochemistry 43, 13510–13524. [PubMed: 15491158]

[58]. Drake EJ, Nicolai DA, and Gulick AM (2006) Structure of the EntB multidomain nonribosomal peptide synthetase and functional analysis of its interaction with the EntE adenylation domain, Chem Biol 13, 409–419. [PubMed: 16632253]

[59]. Reimer JM, Aloise MN, Harrison PM, and Schmeing TM (2016) Synthetic cycle of the initiation module of a formylating nonribosomal peptide synthetase, Nature 529, 239–242. [PubMed: 26762462]

[60]. Bloudoff K, and Schmeing TM (2017) Structural and functional aspects of the nonribosomal peptide synthetase condensation domain superfamily: discovery, dissection and diversity, Biochim Biophys Acta 1865, 1587–1604.

[61]. Stachelhaus T, Mootz HD, and Marahiel MA (1999) The specificity-conferring code of adenylation domains in nonribosomal peptide synthetases, Chem Biol 6, 493–505. [PubMed: 10421756]

[62]. Duckworth BP, Wilson DJ, and Aldrich CC (2016) Measurement of Nonribosomal Peptide Synthetase Adenylation Domain Activity Using a Continuous Hydroxylamine Release Assay, Methods Mol Biol 1401, 53–61. [PubMed: 26831700]

[63]. Hegazi MF, Borchard RT, and Schowen RL (1976) Letter: SN2-like transition state for methyl transfer catalyzed by catechol-O-methyl-transferase, J Am Chem Soc 98, 3048–3049. [PubMed: 1262638]

[64]. Linscott JA, Kapilashrami K, Wang Z, Senevirathne C, Bothwell IR, Blum G, and Luo M (2016) Kinetic isotope effects reveal early transition state of protein lysine methyltransferase SET8, Proc Natl Acad Sci U S A 113, E8369–E8378. [PubMed: 27940912]

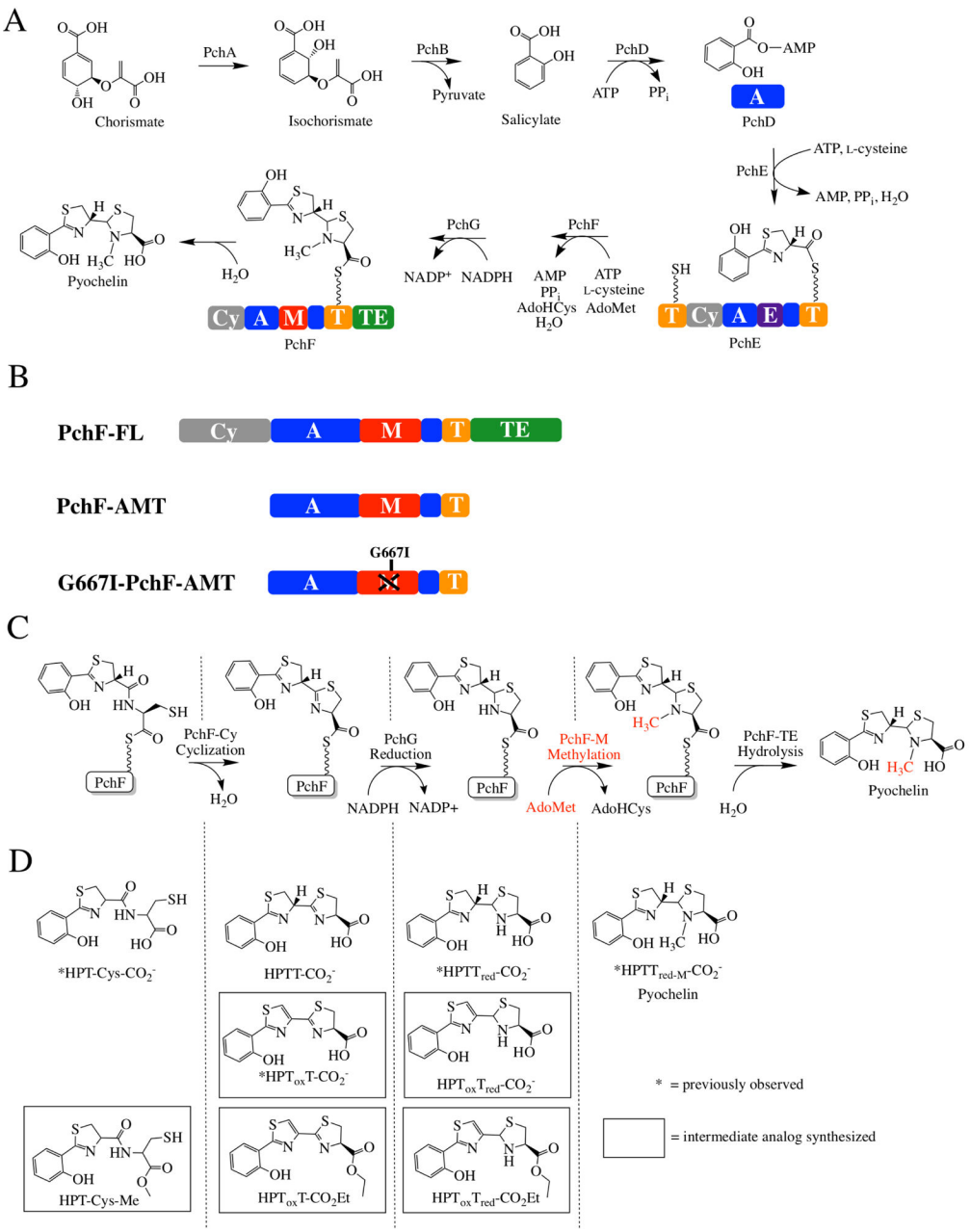

Figure 1: Synthesis of pyochelin.

A) Biosynthetic pathway for pyochelin production. PchA, an isochorismate synthase, and PchB, an isochorismate pyruvate lyase, convert chorismate to salicylate. PchD-G consists of 12 different domains constituting three NRPS modules with three tailoring domains. Together, they assemble pyochelin from salicylate and two L-cysteines, with co-substrates AdoMet, ATP, and NADPH. AdoMet = *S*-adenosylmethionine, AdoHcys = *S*-adenosylhomocysteine. PchD is a stand-alone adenylation domain (A; blue). PchE has *N*- and *C*-terminal thiolation domains (T; yellow), a cyclization domain (Cy; grey), an adenylation domain (A; blue) and a stuffed epimerase domain (E; purple). PchG is a stand-alone NADPH-dependent reductase. PchF is a full-NRPS module consisting of 5 different

domains: a cyclization domain (Cy; grey), adenylation domain (A; blue), stuffed methyltransferase tailoring domain (M; red), thiolation domain (T; yellow), and thioesterase domain (TE; green). **B)** PchF-FL refers to the "full-length" protein, whereas PchF-AMT only includes the stuffed adenylation methyltransferase didomain and the thiolation domain. G667I-PchF-AMT has a mutation to the proposed AdoMet binding domain of the variant PchF-AMT. **C)** The proposed order of chemistries performed by PchF. PchF incorporates L-cysteine to the growing peptide chain. The Cy-domain of PchF continues chain elongation by generating a peptide bond between L-cysteine and the upstream hydroxyphenyl-D-thiazoline moiety of PchE (an intermediate attached to the Ppant of the T-domain of PchE). The Cy-domain then cyclizes the cysteine to form a hydroxyphenyl-(D)-thiazoline-(L)-thiazoline intermediate. PchG (green) reduces the terminal thiazoline of the hydroxyphenyl-bis-heterocycle to thiazolidine using NADPH. The stuffed methyltransferase domain of PchF catalyzes the AdoMet-dependent methyl transfer (highlighted in red) onto the nitrogen of the newly reduced thiazolidine ring before transferring the complete heterocyclic siderophore to the TE-domain releasing the fully mature pyochelin by hydrolysis in the TE-domain. The alternate synthetic schemes where methyl transfer occurs at a different position in the sequence of biosynthesis are shown in Figure S1. **D)** During reconstitution assays, premature hydrolysis releases peptidyl intermediates during biosynthesis. Intermediates previously recovered by Walsh and colleagues are noted with an asterisk. Intermediate analogs used as potential substrates in this study are surrounded by a square. Nomenclature of intermediates is as follows: HP, hydroxyphenyl; T_{ox}, thiazole; T, thiazoline; T_{red}, thiazolidine; CO_2- carboxyl; Et, ethyl; Me/M, methyl.

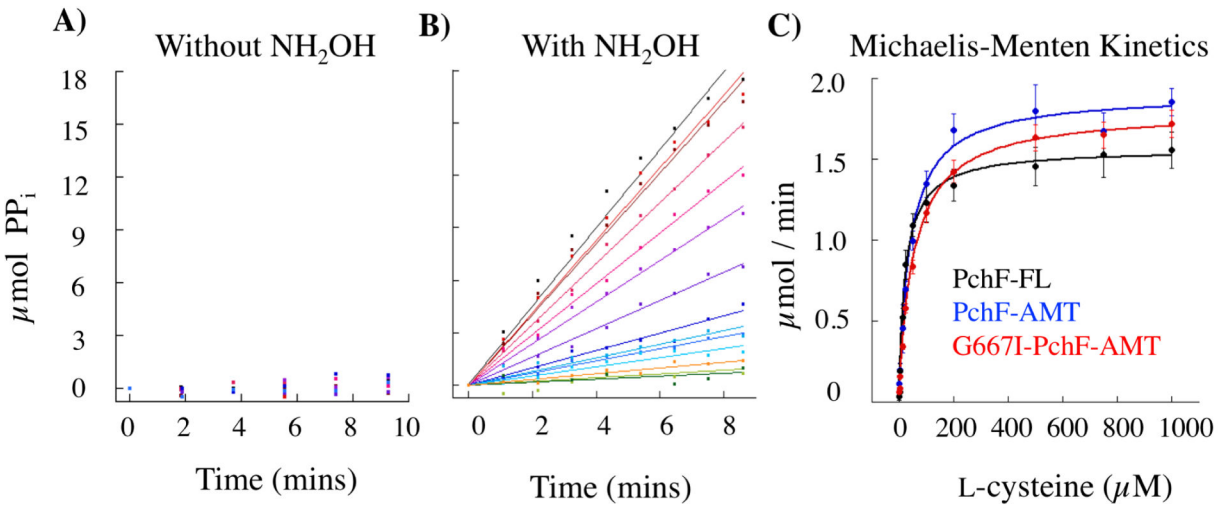

Figure 2: Adenylation activity of PchF variants.

PchF catalyzes the adenylation of L-cysteine by ATP forming an aminoacyl-adenylate bond, releasing pyrophosphate. In the adenylation assay (Figure S3), pyrophosphate is converted to two inorganic phosphates by inorganic pyrophosphatase. 7-methylguanosine is then phosphorylated by purine nucleoside phosphorylase to generate 7-methylguanine, which absorbs at 360 nm. **A)** PchF variants do not turnover with L-cysteine and ATP **(A)**, but do with the addition of hydroxylamine as a nucleophilic surrogate **(B)**. Michaelis-Menten steady-state kinetics **(C)** were performed to compare the L-cysteine adenylation activity of PchF-FL, PchF-AMT, and the methyltransferase null mutant of G667I-PchF-AMT.

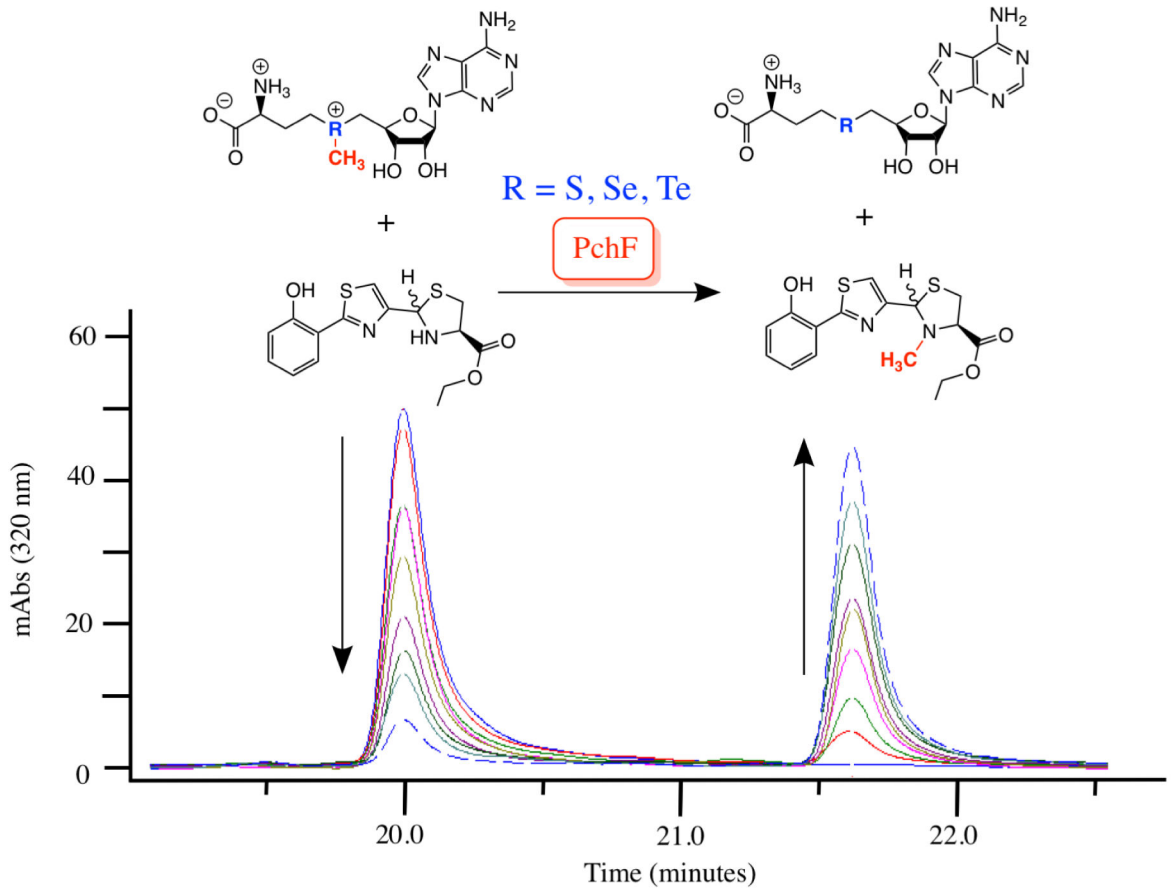

Figure 3: Methylated Product Formation Assay.

PchF catalyzes methyl transfer from its natural co-substrate AdoMet to the synthesized substrate analog, $HPT_{ox}T_{red}$-CO_2Et. Steady-state Michaelis-Menten kinetics were performed by a discontinuous assay. Substrate analog (eluting at 20 min) and product analog (eluting at 21.6 min) were separated by a C18 column using HPLC.

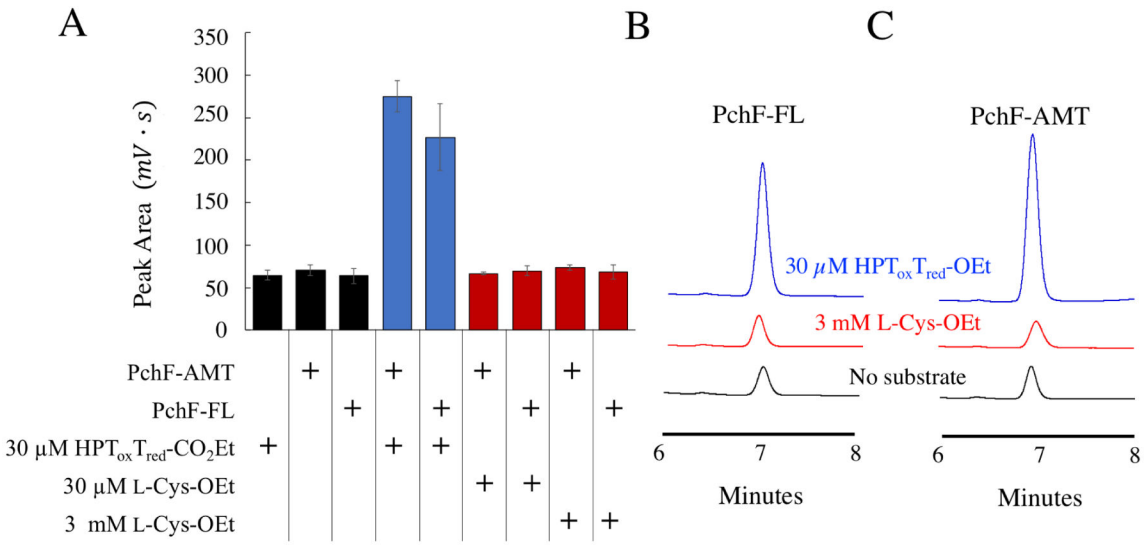

Figure 4: *S*-adenosylhomocysteine Formation Assay.

An orthogonal assay was used to determine if L-Cys-OEt was a substrate analog of PchF methyl transfer by detecting the formation of coproduct, AdoHCys, by UPLC separation. PchF-FL or PchF-AMT was incubated with 1 mM AdoMet and either no substrate, 30 µM $HPT_{ox}T_{red}$-CO_2Et (blue), or 30 µM or 3 mM L-Cys-OEt for 3 hours before being separated by UPLC. **A)** A bar graph showing the peak area quantitation of AdoHCys for reactions with 1) 30 µM $HPT_{ox}T_{red}$-CO_2Et but without enzyme; 2) 1 µM PchF-AMT without substrate; 3) 1 µM PchF-FL without substrate; 4) 1 µM PchF-AMT with 30 µM $HPT_{ox}T_{red}$-CO_2Et; 5) 1 µM PchF-FL with 30µM $HPT_{ox}T_{red}$-CO_2Et; 6) 1 µM PchF-AMT with 30 µM L-Cys-OEt; 7) 1 µM PchF-FL with 30 µM L-Cys-OEt; 8) 1 µM PchF-AMT with 3 mM L-Cys-OEt; and 9) 1 µM PchF-FL with 3mM L-Cys-OEt. Comparative UPLC traces for reactions using **B)** PchF-FL and **C)** PchF-AMT are displayed when using no substrate (black), 3mM L-Cys-OEt (red), and 30 µM $HPT_{ox}T_{red}$-CO_2Et (blue). AdoHCys formation is within error of negative controls when L-Cys-OEt is used as a substrate. In contrast, equimolar amounts of AdoHCys are generated when $HPT_{ox}T_{red}$-CO_2Et is used as a substrate analog.

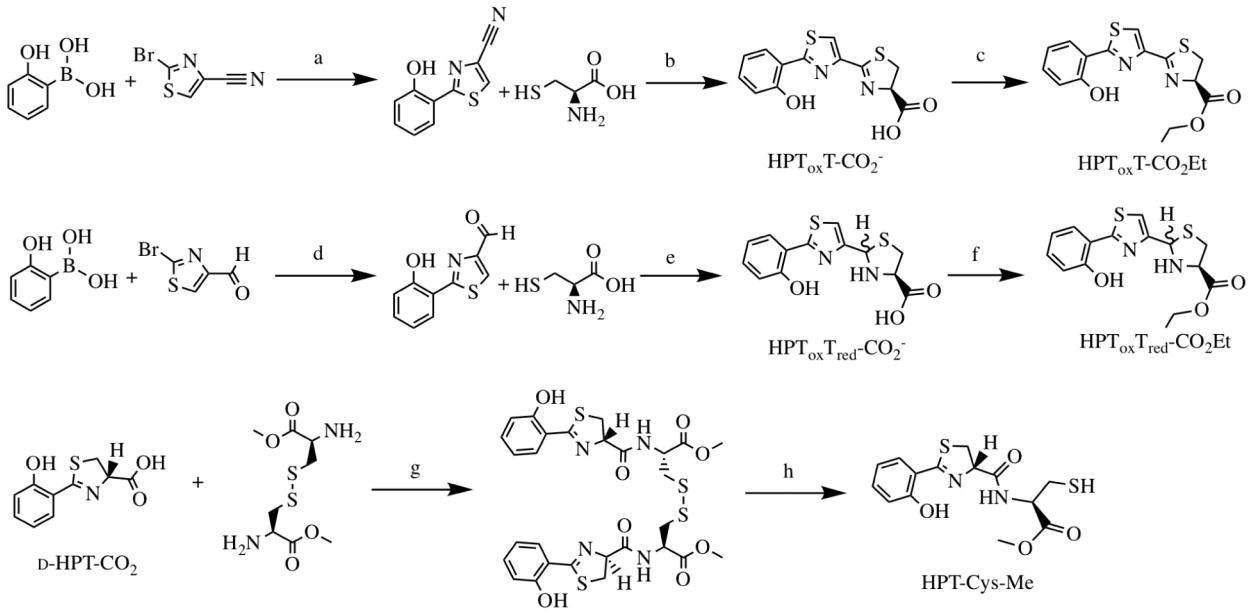

Scheme 1: Substrate analog synthesis of $HPT_{ox}T\text{-}CO_2^-$ $HPT_{ox}T\text{-}CO_2Et$, $HPT_{ox}T_{red}\text{-}CO_2^-$ $HPT_{ox}T_{red}\text{-}CO_2Et$ and HPT-Cys-Me.

Substrate analogs were generated to assess the methyltransferase capabilities of PchF. Reagents and conditions: a) $Pd(PPh_3)_4$, K_2CO_3/DME, H_2O, 150 °C, 49%;[42] b) MeOH, K_2HPO_4(aq) (pH 6.5), 60 °C, 70%;[42] c) $SOCl_2$/EtOH, 40 °C, 49%;[42] d) $Pd(PPh_3)_4$, K_2CO_3/DME, H_2O, 100°C, 70%; e) EtOH/KCO_2CH_3 (aq), RT, 95%; f) $SOCl_2$/EtOH, 40°C, 55%; g) DIEA, COMU/DMF, 0°C 1hr, RT 3hr, 12%; h) generated in the presence of 5mM TCEP *in vitro*.

Table 1:

L-Cysteine adenylation assay – kinetic parameters

	PchF-FL[a]	PchF-FL	PchF-AMT	G667I-PchF-AMT
k_{cat} (min^{-1})	415	2.6 ± 0.2	3.2 ± 0.2	3.0 ± 0.3
K_M (L-Cys μM)	537	25 ± 2	41 ± 8	54 ± 6
k_{cat}/K_M($M^{-1}s^{-}$)	13300	1800 ± 200	1300 ± 300	900 ± 100

[a]Quadri, Keating, Patel, Walsh. *Biochemistry* 1999, 38, 14941–14954. Quadri *et al* used an exchange assay measuring the reverse reaction that incorporates ^{32}P-pyrophosphate into ATP.

Table 2:

Methylated product formation assay varying $HPT_{ox}T_{red}$-CO_2Et – kinetic parameters

	PchF-FL	PchF-AMT	G667I-PchF-AMT
k_{cat} (min^{-1})	1.96 ± 0.04	2.9 ± 0.1	Not Detected
K_M (AdoMet μM)	3.6 ± 0.2	7.5 ± 0.2	Not Detected
k_{cat}/K_M ($M^{-1}s^{-1}$)	9100 ± 500	6500 ± 300	Not Detected

Table 3:

Onium chalcogen effects for methyltransferase activity of PchF-FL and PchF-AMT.

Enzyme	Substrate	k_{cat} (min^{-1})	K_M (μM)	k_{cat}/K_M ($M^{-1}s^{-1}$)
PchF-FL	AdoMet	1.2 ± 0.1	3.3 ± 0.8	6000 ± 2000
	SeAdoMet	2.3 ± 0.6	3 ± 1	13000 ± 5000
	TeAdoMet	0.056 ± 0.003	160 ± 10	6.0 ± 0.5
PchF-AMT	AdoMet	2.48 ± 0.04	7.3 ± 0.8	5700 ± 600
	SeAdoMet	5.4 ± 0.8	5.4 ± 0.5	17000 ± 3000
	TeAdoMet	0.054± 0.003	140 ± 20	7 ± 1

Table 4:

Kinetic parameter comparison between AdoMet, SeAdoMet, and TeAdoMet

Enzyme	Substrate Analog	k_{cat} (Se/Te)AdoMet / AdoMet	k_{cat}/K_M (Se/Te)AdoMet / AdoMet
CFA [a] Synthase	SeAdoMet	1.8	2.8
	TeAdoMet	0.50	0.059
COMT [a]	SeAdoMet	1.1	1.2
	TeAdoMet	0.16	0.0089
SET8 [b]	SeAdoMet	1.9	1.9
PchF-FL	SeAdoMet	1.9	2.2
	TeAdoMet	0.047	0.0010
PchF-AMT	SeAdoMet	2.2	3.0
	TeAdoMet	0.022	0.0012

[a] Iwig, Grippe, McIntyre, Booker. *Biochemistry,* 2004, 43, 13510-13524.

[b] Linscott, Kapilashrami, Wang, Senevirathne, Bothwell, Blum, Luo. *Proc. Natl. Acad. Sci.,* 2016, 113, E8369-E8378.